Food & Function

Storage conditions modulate the metabolomic profile of a black raspberry nectar with minimal impact on bioactivity

Journal:	*Food & Function*
Manuscript ID	FO-ART-04-2018-000639.R1
Article Type:	Paper
Date Submitted by the Author:	20-Jun-2018
Complete List of Authors:	Teegarden, Matthew; The Ohio State University, Food Science & Technology Knobloch, Thomas; The Ohio State University, College of Public Health Weghorst, Christopher; The Ohio State University, College of Public Health Cooperstone, Jessica; The Ohio State University, Horticulture and Crop Science; The Ohio State University, Food Science & Technology Peterson, Devin; The Ohio State University, Food Science & Technology

Storage conditions modulate the metabolomic profile of a black raspberry nectar with minimal impact on bioactivity

Matthew D. Teegarden[1], Thomas J. Knobloch[2], Christopher M. Weghorst[2], Jessica L. Cooperstone[1,3*], Devin G. Peterson[1]

[1]Department of Food Science and Technology, The Ohio State University, Columbus, OH, USA

[2]College of Public Health, Division of Environmental Health Sciences, The Ohio State University, Columbus, OH, US

[3]Department of Horticulture and Crop Science, The Ohio State University, Columbus, OH, USA

*Cooperstone.1@osu.edu

Abstract

Pre-clinical and clinical studies suggest black raspberries (BRBs) may inhibit the development of oral cancer. Lyophilized BRB powder is commonly used in these studies, but processed BRB products are more often consumed. The objective of this work was to understand how storage conditions influence the phytochemical profile and anti-proliferative activity of a BRB nectar beverage. Untargeted UHPLC-Q-TOF-MS based metabolomics analyses demonstrated that large chemical variation was introduced by storage above -20 °C over 60 days. However, minimal change in anti-proliferative activity was observed when stored nectar extracts were applied to SCC-83-01-82 premalignant oral epithelial cells. As proof of concept, cyanidin-3-*O*-rutinoside and its degradation product, protocatechuic acid, were administered in different ratios maintaining an equimolar dose, and anti-proliferative activity was maintained. This study shows the utility of metabolomics to profile global chemical changes in foods, while demonstrating that isolated phytochemicals do not explain the complete bioactivity of a complex food product.

1. Introduction

Black raspberries (BRBs) are extensively studied for their cancer preventative properties [1,2]. Their bioactivity has been attributed to their rich phytochemical profile inclusive of anthocyanins, ellagitannins, organic acids, and quercetin among other phenolic compounds [3]. It has been hypothesized that these components elicit a complex series of biological responses that result in a net inhibition of cancer growth [4]. Because of their high concentration of phenolic compounds, BRBs have been the subject of many studies on food-based chemoprevention strategies.

Much of the interest in the chemopreventative properties of BRBs has focused on oral cancer [5–9]. The oral cavity presents unique opportunities for chemoprevention through dietary means due to direct exposure of tissues to food phytochemicals. Oral cancer is prevalent throughout the world, with higher incidence observed in men and people in less developed regions [10,11]. The majority of oral cancers are squamous cell carcinomas (SCCs), and risk factors include tobacco use, alcohol consumption, human papillomavirus infection, and chronic periodontal disease [12]. Pre-clinical models have consistently shown reduction of oral SCC incidence and multiplicity using whole freeze-dried BRBs, likely due to engagement of a number of biological mechanisms [13]. A human clinical trial with a BRB-based mucoadhesive gel demonstrated the ability of BRBs to reduce the size and severity of precancerous oral lesions [8], while a relative reduction in the expression of molecular biomarkers indicative of SCC was observed after patients were treated with BRB-based troches for two weeks [6]. These studies support a role for BRB-mediated efficacy in oral cancer prevention strategies.

Most research using BRBs has been conducted with minimally processed, lyophilized BRB powder. In practical terms, consumers mostly encounter BRBs after they have been

incorporated into shelf-stable food products and stored for varying lengths of time, during which the phytochemical profile may be altered [14]. Research on the stability of the phytochemical profile in BRB-based food products is limited to a short defined list of compounds [14–16], while effects on the global phytochemical profile and bioactivity of these products are unknown. Metabolomics is an emerging approach to chemical analysis in which hundreds to thousands of compounds within a food system are profiled, with the potential to provide new insight into the relationship between food phytochemicals and health outcomes [17]. The objective of the current study is to use an untargeted metabolomics approach to understand the global differences in the phytochemical profile of a BRB nectar beverage over storage time and temperature variations, and how these changes relate to the growth inhibition activity in an *in vitro* oral premalignacy model.

2. Experimental

2.1 Chemicals

All solvents were of HPLC-MS grade from Fischer Scientific (Pittsburgh, PA) unless otherwise noted. Cyanidin-3-*O*-rutinoside (C3R) and protocatechuic acid (PA) standards were from Sigma Aldrich (St. Louis, MO). Cell culture-grade dimethyl sulfoxide and water were also from Sigma Aldrich.

2.2 Nectar Processing, Storage, and Sampling

Nectar was prepared in the pilot plant facilities located at The Ohio State University (Columbus, OH) using a formula similar to that described by Gu and colleagues, as shown in Table 1 [16]. The BRB powder used was produced from whole BRBs harvested at Stokes Berry

Farm (Wilmington, OH). All components were combined in a high shear mixer for 20 min, and the nectar was subsequently pasteurized using a MicroThermics UHT/HTSTLab-25HV Hybrid unit (MicroThermics, Inc., Raleigh, NC, USA). The processing specifications mirrored industry practices for pasteurization of this product by which the nectar was held at 100 °C (± 1.1 °C) for 23 sec, immediately cooled, and aseptically filled into pre-sterilized 50 mL conical centrifuge tubes.

Nectar was stored at -20 °C, 4 °C, 10 °C, 25 °C, or 35 °C for 60 d with samples (n=4) removed from each condition at 5 d, 10 d, and subsequently in 10 d intervals. Two months has been described as an appropriate amount of time to study stability in foods intended for clinical trials, as time is often needed for subject recruitment and intervention [16]. At each time point the nectar was centrifuged (1000 x *g*) for 5 min, partitioned into smaller aliquots, and stored at -80 °C prior to use. Samples of freshly produced nectar were also stored at -80 °C at the time of production as a t_0 sample. Aerobic plate counts and yeast and mold counts were obtained for the 35 °C incubated samples at each time point with 3M Petrifilm (3M Company; Maplewood, MN), according to manufacturer instructions.

2.3 Sample Preparation and Analysis for Untargeted Metabolomics

Aliquots (1 mL) of nectar were thawed in a room temperature water bath for 10 min. Once thawed, 750 µL were deposited into a glass vial followed by 2.25 mL of 0.1% formic acid in methanol. The mixture was homogenized with a probe sonicator (Branson Ultrasonics; Danbury, CT) for 10 sec and centrifuged for 5 min at 1000 x *g* (4 °C). The supernatant was decanted into a glass vial, and the pellet was extracted twice more with 3 mL of 75% methanol in

97 water with 0.1% formic acid. Aliquots (200 μL) were deposited into 4 mL glass vials, dried
98 under a stream of nitrogen, and stored at -20 °C until analysis.
99 Dried aliquots were solubilized in 100 μL 25% methanol in water with 0.1% formic acid
100 and vortexed for 15 sec. Samples were then centrifuged at 21,130 x *g* for 4 min (4 °C) and placed
101 in the autosampler of a 1290 Infinity II series UHPLC (Agilent Technologies, Santa Clara, CA)
102 maintained at 4 °C until analysis. Samples were injected (5 μL) onto a 2.1 x 100 mm, 1.8 μm
103 Acquity HSS T3 column (Waters, Milford, MA) maintained at 40 °C. The mobile phase
104 consisted of A: 0.1% formic acid in water and B: 0.1% formic acid in acetonitrile with a flow
105 rate of 0.5 mL/min. The linear gradient program was as follows: 0% B held for 1 min, increased
106 to 60% B over 5 min, increased to 100% B over 2 min and hold for 1.5 min, immediately
107 switched to 0% B and held for 2 min for a total run time of 11.5 min.
108 Eluent was directed to an Agilent iFunnel 6550 QTOF-MS interfaced with an
109 electrospray ionization (ESI) source operated in negative ion mode. The first minute of flow
110 from the UHPLC was directed to waste. Relevant MS settings were as follows: gas temp 150 °C,
111 drying gas 18 L/min, nebulizer 30 psig, sheath gas temp 350 °C, sheath gas flow 12 L/min, VCap
112 4000 V, nozzle voltage 2000 V, acquisition mode was 2 GHz extended dynamic range with a
113 mass range of 50–1700 m/z. Reference mass solution (Agilent Technologies) was concurrently
114 infused into the source via a dedicated sprayer for continual mass correction. Sample run order
115 was randomized. Quality control samples, composed of equal portions of each nectar sample,
116 were run every 10 samples to monitor instrument performance over the run time (data not
117 shown).
118
119 *2.4 Data Pre-processing and Analysis for Untargeted Metabolomics*

120 Raw spectral data was processed using the batch recursive feature extraction algorithm in
121 Profinder (B.08.00, Agilent Technologies). Mass spectral features were picked and binned
122 according to expected isotope patterns, adducts, and charge states. These molecular features were
123 then aligned across all samples, and those appearing in less than three samples per
124 time/temperature group were removed from further analysis. The raw data was then searched
125 against this assembled list in a targeted manner to improve the quality of the data used for
126 multivariate analysis. Further data pre-processing was performed in Mass Profiler Professional
127 (version 14.5, Agilent Technologies), including removal of features present in sample blanks. To
128 remove low quality peaks from the data, an additional abundance filter was applied which
129 required a minimum peak height of 5.0×10^4 in 75% of the samples in at least one
130 time/temperature sample group.
131 Multivariate analyses, including principal component analysis and partial least squares
132 regression (PLS), were executed in R (version 3.2.3) with the ropls package using the autofit
133 option to determine the optimal number of components[18]. Data were $\log_{10}$ transformed and
134 Pareto scaled prior to analysis. PCA is a dimensional reduction technique that allows for analysis
135 of multidimensional data in an easily-visualized space. PLS is a common multivariate modeling
136 technique that builds off the dimensional reduction properties of PCA but in the framework of a
137 linear regression [19]. Separate PLS models were constructed for each storage condition. The X
138 matrices were composed of features present in 75% of replicates from at least one time point in
139 each storage condition, and the Y matrix was storage time. Performance of the PLS models was
140 assessed using 8-segment cross validation, and statistical significance of each model was
141 determined using permutation tests (n = 100). Features with a variable importance on projection
142 value (VIP) ≥ 1 across all successful models were manually reviewed before further analysis.

Similarly, features with a VIP ≥ 1 in only the 35 °C samples were also manually reviewed for further analysis. VIP scores are estimates of the relative importance of a chemical feature to a given PLS model, and features with a score ≥ 1 are typically considered to be important in the model. A data pre-treatment and analysis summary is shown in Figure 1.

2.5 Targeted Compound Analysis

Cyanidin-3-*O*-rutinoside (C3R) and protocatechuic acid (PA) were quantified in the nectar samples from t_0 and 60d at 35 °C. Extracts of BRB nectar were obtained as described for the untargeted metabolomics workflow, reconstituted in 5 mL of 5% aqueous formic acid, and filtered through a 0.22 μm nylon filter. Samples were then injected (0.5 μL) into an Agilent 1290 Infinity II UHPLC coupled to an Agilent 6495 triple quadrupole MS equipped with an ESI source operated in positive and negative ion modes. The mobile phase consisted of A: 5% aqueous formic acid and B: 5% formic acid in acetonitrile. The column and gradient program were identical to that was described here for untargeted analyses. MS parameters included gas temp: 150 °C, gas flow: 18 L/min, nebulizer: 45 psi, sheath gas heater: 375 °C, sheath gas flow: 12 L/min, capillary: 3000 V, fragmentor: 350. Quantitation was performed using standard curves constructed from serial dilutions of authentic standards. The transitions used for each compound were as follows: C3R: 595 [M+] → 287 (CE = 17 V), PCA: 153 $[M-H]^-$ → 109 (CE = 10).

2.6 Extract Preparation for Cell Study

Extraction of the nectar was scaled up from the procedure used in the untargeted metabolomics workflow to ensure sufficient extract mass. Briefly, nectar replicates were pooled and 1 mL aliquots were deposited into glass vials followed by 3 mL of 0.1% formic acid in

166 methanol. The mixture was homogenized with a probe sonicator and centrifuged at 3220 × *g* (4
167 °C) for 7 min. The supernatant was decanted into a glass vial, and the pellet was extracted once
168 with 75% aqueous methanol with 0.1% formic acid. The pooled supernatants were dried using a
169 Genevac EZ2 vacuum evaporation system (SP Scientific; Ipswich, United Kingdom) set at 30
170 °C. Remaining water was removed by lyophilization on a Labconco FreeZone 12 Plus system
171 (Kansas City, MO). Nectar extracts were reconstituted in 1:1 DMSO/water, sonicated for 15 sec,
172 and diluted to a concentration of 2 mg extract/mL in cell culture media.
173
174 *2.7 Cell Culture and Growth Inhibition Assay*
175 Premalignant human oral epithelial cells (SCC-83-01-82) were maintained in modified
176 minimal essential medium (MEM) with 10% fetal bovine serum and 5% antibiotic/antimycotic
177 solution including penicillin (10,000 U/mL), streptomycin (10,000 U/mL), and amphotericin B
178 (25 μg/mL) as previously described [20,21]. The characteristics of this cell line have been previously
179 described [22]. Cell cultures were incubated at 37 °C in a 90% humidified environment with 5%
180 CO_2 atmosphere.
181 Cells were seeded at a density of 1000 per well in 96-well plates. After 24 hr, the media
182 was replaced to deliver 200 μg extract/well or standards of C3G or PA at concentrations ranging
183 from 3–100 μg/mL using previous work with crude berry product extracts and their isolated
184 components as a guide [23]. Control samples were composed of an equivalent amount of 1:1
185 DMSO/water diluted in MEM. All samples were incubated for 72 hr.
186 Growth inhibition was determined using a WST-1 assay (Roche; Pleasanton, CA)
187 according to manufacturer instructions. Growth inhibition was calculated as $1 - ((A_{trt}-A_{trt\ blank})/(A_{control}-A_{control\ blank}))$. Treatment blanks were made by incubating sterile media with the
188

corresponding dose of nectar extracts or phytochemicals in identical conditions as the treated cells. Technical replicates were performed in quadruplicate, while biological replicates were performed in triplicate. Cytotoxic activity was evaluated using the Clontech LDH Cytotoxicity Detection Kit (Mountain View, CA) according to manufacturer instructions. Data were analyzed using the generalized linear model procedure in SAS version 9.4. The data were fitted with an ANOVA model with terms corresponding to nectar incubation time, temperature, and their interaction with significance reported at $P<0.05$. Differences between treatments were assessed using Tukey's post hoc test with $\alpha = 0.05$.

3 Results and Discussion

We report on the phytochemical stability of a BRB nectar over storage using targeted and untargeted metabolomics, and we relate these chemical changes to their bioactive properties on premalignant oral epithelial cell proliferation. The product was a viscous liquid with pH of 3.4 and soluble solids reading of 9 °Brix. Microbial growth observed during storage was below the limit of quantitation (data not shown), indicating that any chemical changes incurred over storage were not due to microbial metabolism. Untargeted metabolomics has been used by others to understand the chemistry of foods in several applications including food authentication, effects of different production practices, the dynamics of fermentation processes, and recently, changes in flavor attributes during storage [24–26]. Here we use the technique to understand how the chemistry of BRB nectar, as impacted by storage, may relate to the biological activity of the product.

3.1 Untargeted Metabolomics Revealed Large Chemical Variation with Elevated Storage Temperatures

Full scan UHPLC-MS-QTOF data was acquired for all nectar samples. Following the extraction, alignment, binning, and filtering of peaks in the data, a total of 1,712 molecular features were considered for further analyses. Overall trends across the dataset were visualized using principal component analysis (PCA) autofitted to three components. Only the first two comonents are displayed in Figure 2 to simplify data interpretation, as the third component only explained 3.8% of the variation. The scores plot in Figure 2 indicates that the samples stored at -20 °C were relatively stable over 60 days of storage as demonstrated by their close clustering and proximity to the samples from t_0. Samples stored at higher temperatures for longer amounts of time were further separated from the t_0 samples along the first component, which explained 37.7% of the variation, suggesting that considerable chemical variation was introduced with elevated temperature and time.

Partial least squares regression (PLS) was used to further understand how chemical profiles of BRB nectars stored at different temperatures changed over time. A separate model for each storage temperature was generated in which relative feature abundances were regressed against storage time, including t_0 (Table 2). The model for samples stored at -20 °C was of poor quality ($Q^2 = 0.165$; $P = 0.03$), indicating that storage time was not a strong predictor of chemical variation in these samples. This further demonstrated the stability of BRB nectar stored at -20 °C for 60 d. The models for samples stored at 4 °C–35 °C all had a $Q^2 > 0.9$ ($P = 0.01$), which indicated good performance of these models. We focused our analysis on features that were influenced by storage time, regardless of storage temperature, by collating features with VIP ≥ 1 across all four PLS models. Following a manual data quality review, 73 features were

found to contribute significantly to all four models. Figure 3 displays the mean relative abundance of these features at each time point across storage conditions. Features were clustered using Euclidian distance metric and Ward's linkage rule. The heat map demonstrates that these significant features increased and decreased simultaneously at storage temperatures above -20 °C. These relative changes in abundance appeared to be more severe at 25 °C and 35 °C storage, as anticipated. The features in cluster A reflect a pattern of formation by which features were not present at t_0 and were created over time, more so at higher temperatures. At 35 °C, some of these features decreased in abundance before day 60, indicating further degradation of these generated compounds. Cluster B contains features that degraded over time, some which degraded after 20 days at 35 °C. The features in cluster C increased in abundance continuously over time with elevated storage temperatures. Many of these features were present at low levels in the t_0 samples. These data demonstrate that above -20 °C, the BRB nectar is a system in dynamic chemical flux over 60 days of storage.

Tentative identifications were generated for some features based on plausible database matches from FooDB (www.foodb.ca), a component of the human metabolome database [27]. Identities were confirmed by authentic standards or by collecting additional MS/MS fragmentation data and comparing to published values when authentic standards were unavailable. These techniques correspond to identification levels 1 and 2, respectively, as proposed by the Metabolomics Standard Initiative [28]. Table 3 displays features that were identified using these methods, all of which have been previously reported in BRBs [29]. Catechin and epicatechin are isomeric flavan-3-ols, and their levels have been shown to decline over storage in other products such as apple juice [30], and a variety of blueberry products [31]. B-type procyanidins are oligomers of catechin and/or epicatechin linked by C-C bonds, and have also

257 been reported to be unstable over storage [31]. The MS/MS fragmentation patterns of the B-type
258 procyanidins from the current work closely resembled those reported previously [32]. PA is a B-
259 ring cleavage product of cyanidin-based anthocyanins that can form as a result of heating or
260 storage, but is also present in fresh BRBs [29,33].

261 The lack of plausible database matches for many of the features in clusters A and C in
262 Figure 3 led us to hypothesize that these entities may be uncharacterized degradation products of
263 BRB components. The Maillard reaction is a prevalent reaction between reducing sugars and
264 amino acids that occurs over processing and storage of foods. Intermediates in this reaction
265 include reactive carbonyl species that can form adducts with phenolic compounds, such as
266 epicatechin, in food products [34]. Kokkinidou and Peterson demonstrated that phenolic-reactive
267 carbonyl species adducts can be decomposed by derivatization with *o*-phenylenediamine [35].
268 When *o*-phenylenediamine was added to BRB nectar extracts, the abundances of 7 features from
269 clusters A and C in Figure 3 were significantly or completely reduced, suggesting that these may
270 be Maillard-related sugar fragmentation-phenolic degradation products.

271

272 *3.2 All Extracts of Stored BRB Nectar Inhibited* SCC-83-01-82 *Cell Growth Similarly*

273 BRB nectar extracts were applied to SCC-83-01-82 premalignant oral epithelial cells to
274 assess the effects of storage time and temperature on their cell growth activities. Extracts of the t_0
275 nectar samples inhibited cell growth 27.8 ± 2.8% with inhibition of the stored samples shown in
276 Figure 4. Data were evaluated using a two-way ANOVA model including terms for nectar
277 storage time, temperature, and their interaction. The terms for time ($P < 0.01$), temperature ($P <$
278 0.01), and their interaction ($P<0.0001$) were significant. Few significant differences, however,
279 were seen across time within any one storage condition, except for a 13% difference between

samples stored for 10, 20, and 60 days at 35 °C (Figure 4). Non-significant trends emerged in the dataset, but were inconsistent among storage conditions. For example, a non-significant decrease in cell growth activity was observed for nectars stored at 10 °C, but this same trend was not maintained with storage at 25 °C. Thus, the capacity of BRB nectar extracts to inhibit SCC-83-01-82 cell growth after 72 hr of incubation was relatively unaffected by nectar storage conditions, despite the large variation seen in the nectar chemical profiles.

Few studies have investigated the relationship between storage conditions of berry products, their corresponding chemical profiles, and bioactivity. A decrease in total anthocyanin content was observed over 60 days in blueberry juice produced from two different cultivars and stored at 6 °C and 23 °C. When the anthocyanin fraction of the juice was isolated and applied to HT-29 colorectal adenocarcinoma cells, the authors observed significant decreases in anti-proliferative activity after 30–90 days of storage. Only a slight decrease in anti-proliferative activity was noted in samples stored at 23 °C for 60 days, but it was concluded that storage conditions influenced the anthocyanin profiles and biological activities of the juices [36]. The untargeted metabolomics approach employed in the present work aims to elucidate the relationship between the chemical profile and biological activity of a berry product in a more comprehensive way. BRBs contain a complex mixture of phytochemicals, thus it is unlikely that any single chemical component can account for the complete bioactivity of the fruit. For example, feeding whole BRB powder, anthocyanin-rich BRB extract, or anthocyanin-deplete extract all suppressed the growth of tumors to an identical amount in a rat model of esophageal cancer [37]. Paudel and colleagues used NMR-based metabolomics to understand the effects of BRB cultivar and degree of ripeness on bioactivity in HT-29 colon cancer cells. They observed a myriad of biologically active BRB components including anthocyanins, other flavonoids, organic

303 acids, and ellagic acid derivatives [38]. Our data support these findings in that we observed
304 nominal changes in bioactivity of BRB nectar products with considerably different
305 phytochemical profiles, further demonstrating that a number of phytochemicals are responsible
306 for this bioactivity.
307
308 *3.3 C3R and its degradation product PA Equally Contribute to the Bioactivity of BRB Nectar*
309 Since the anti-proliferative activity of stored nectars was relatively unchanged despite
310 large changes in chemical profiles, we hypothesized that parent phytochemicals, as well as their
311 degradation products, both contribute to the bioactivity of the product due to similarity in
312 structural motifs. Anthocyanins constitute a large portion of the total polyphenols of BRBs, with
313 C3R as a predominant species [39–41]. Given that PA is a reported degradation product of C3R and
314 was identified as an important feature in our PLS models, we focused on these two compounds
315 in a model system as proof-of-concept that parent compounds and their associated degradation
316 products can be complementarily bioactive.
317 To understand how these two related compounds changed in the nectar over time, we
318 extracted information about their abundances from the untargeted UHPLC-MS-QTOF dataset
319 (Figure 5). The relative change in abundance over time was greater at higher storage
320 temperatures for both compounds, consistent with prior findings on anthocyanin degradation [42].
321 C3R and PA were subsequently quantitated at t_0 and 60 d of storage at 35 °C using UHPLC-
322 MS/MS and authentic standard curves (Table 4). Interestingly, C3R decreased by 13.1 nmol/mg,
323 while PA increased by 14.9 nmol/mg during storage, demonstrating that these two bioactive
324 compounds exchanged in near-equimolar amounts in the BRB nectar. It must be noted that

anthocyanins can degrade via a multitude of mechanisms to form several different products apart from PA, while PA can also be a degradation product from other phenolics [42]

Independently, C3R and PA each inhibited the growth of SCC-83-01-82 cells in a dose-dependent manner (Figure 6A, B), with increasing concentrations corresponding with increased growth inhibition. The growth inhibition by C3R is similar to levels previously reported on cyanidin-3-*O*-glucoside isolated from strawberries, which inhibited the growth of CAL-27 malignant oral cancer cells by approximately 50% at a level of 100 μg/mL (222 μmol/L) [43]. The current work further validates the bioactivity of cyanidin-based anthocyanins to inhibit cell growth in human oral cell lines. The anticancer activity of PA against oral cancer has previously been demonstrated in animal models [44]. While the concentrations we tested *in vitro* are higher than those found in the BRB nectar, our results show that SCC-83-01-82 cells respond to individual treatments of C3R or PA in a dose-dependent manner.

To demonstrate that BRB phytochemicals and their degradation products can each contribute to the biological activity of the nectar, we delivered doses of equal molarity but differing molar ratios of C3R:PA. The conditions used mirror the equimolar exchange of these two compounds observed in the nectar. As shown in Figure 6C, after a starting dose of 170 μmol/L, C3R was reduced by 25% in successive treatments, while in parallel the concentrations of PA were increased in 25% increments to a final treatment dose of 170 μM. A consistent level of growth inhibition was maintained across treatments ($P = 0.092$ for differences among treatments) despite differing molar ratios of C3R:PCA. Consequently, our data demonstrates that the loss in bioactivity of a parent phytochemical (C3R) may be recovered by increased levels of their degradation products (PA) (Figure 6C). Previous studies with other cancer models have found the ortho-dihydroxyphenyl structural element of some anthocyanidins, such as cyanidin, to

348 be critical for anti-cancer properties of these compounds [45]. Our data suggest that this structural
349 moiety, the main molecular structure maintained between C3R and PA, may also play a role in
350 suppressing the growth of SCC-83-01-82 cells. Partial degradation of cyanidin-3-glucoside in
351 cell culture media has been previously reported, with PA as the primary degradation product [46].
352 While this represents an inherent limitation of studying anthocyanins *in vitro*, it further validates
353 the idea that phytochemical degradation products can maintain active chemical moieties, and
354 thus bioactivity.. We speculate that this phenomenon of degrading phytochemicals while
355 maintaining active chemical moieties occurs on a larger scale with other components of the
356 nectar. Additionally, it is plausible that phytochemicals that remain unchanged throughout
357 storage contribute significantly to bioactivity. And while not addressed in the current study, it is
358 also conceivable that the biochemical signaling and activation mechanisms underlying the
359 growth inhibition shifted with changing nectar chemical profiles. In addition, our bioassay was
360 an *in vitro* model with oral cells that can be directly exposed to BRB phytochemicals *in vivo*.
361 Not addressed in this study is the impact that storage-induced changes in BRB phytochemicals
362 affects their bioaccessibility and bioavailability in the remainder of the GI tract, which could
363 have implications for their actions elsewhere in the body.
364

365 **4. Conclusions**

366 We investigated the impact of storage on the phytochemical stability and bioactivity of a
367 BRB nectar product. Our data demonstrate that nectar stored at -20 °C is chemically stable over
368 60 days, but storage above this temperature introduces large amounts of chemical variation
369 through a variety of mechanisms including cleavage of phenolic compounds and potential adduct
370 formation with reactive carbonyl species. Despite the large chemical variation observed using

371 untargeted metabolomics, storage conditions had minimal impact on the ability of the nectar to
372 differentially inhibit growth in premalignant oral epithelial cells. Exploration of this phenomenon
373 *in vitro* supports our hypothesis that degradation products of bioactive phytochemicals also
374 demonstrate bioactivity, allowing maintenance of growth inhibition capacity, through
375 independent, cooperative, or redundant mechanisms. This work demonstrates that BRBs are a
376 complex mixture of compounds with potential anticancer activities. Assigning functional activity
377 to a single black raspberry compound or metabolite fails to explain and appreciate this fluidity,
378 as different compounds increase and decrease with the dynamics of storage. It remains important
379 to dissect these pleiotropic phytochemical bioactives to fully understand the health benefits and
380 consequences of consuming BRBs and their components.
381

382 **Acknowledgements**

383 The authors would like to thank David M. Phinney, M.S. for his assistance in processing the
384 nectar utilized in this study. This work was supported by USDA-NIFA National Needs
385 Fellowship (2014-38420-21844), the Lisa and Dan Wampler Endowed Fellowship for Food and
386 Health Research and Foods for Health, a focus area of the Discovery Themes Initiative at The
387 Ohio State University.
388

389 **Abbreviations Used**

390 BRB: black raspberry; SCC: squamous cell carcinoma; C3R: cyanidin-3-*O*-rutinoside; PA:
391 protocatechuic acid; PLS: partial least squares; PCA: principal components analysis; VIP:
392 variable importance on projection
393

Conflicts of Interest

The authors have no conflicts of interest to declare.

5. References

(1) Kula, M.; Krauze-Baranowska, M. *Nutr. Cancer* **2016**, *68*, 18–28.

(2) Kresty, L. A.; Mallery, S. R.; Stoner, G. D. *J. Berry Res.* **2016**, *6*, 251–261.

(3) Stoner, G. D. *Cancer Prev. Res.* **2009**, *2*, 187–194.

(4) Liu, R. H. *Am. J. Clin. Nutr.* **2003**, *78*, 517S–520S.

(5) Warner, B. M.; Casto, B. C.; Knobloch, T. J.; Accurso, B. T.; Weghorst, C. M. *Oral Surg. Oral Med. Oral Pathol. Oral Radiol.* **2014**, *118*, 674–683.

(6) Knobloch, T. J.; Uhrig, L. K.; Pearl, D. K.; Casto, B. C.; Warner, B. M.; Clinton, S. K.; Sardo-Molmenti, C. L.; Ferguson, J. M.; Daly, B. T.; Riedl, K.; Schwartz, S. J.; Vodovotz, Y.; Buchta, A. J.; Schuller, D. E.; Ozer, E.; Agrawal, A.; Weghorst, C. M. *Cancer Prev. Res.* **2016**, *9*, 159–171.

(7) Oghumu, S.; Casto, B. C.; Ahn-Jarvis, J.; Weghorst, L. C.; Maloney, J.; Geuy, P.; Horvath, K. Z.; Bollinger, C. E.; Warner, B. M.; Summersgill, K. F.; Weghorst, C. M.; Knobloch, T. J. *Front. Immunol.* **2017**, *8*.

(8) Mallery, S. R.; Tong, M.; Shumway, B. S.; Curran, A. E.; Larsen, P. E.; Ness, G. M.; Kennedy, K. S.; Blakey, G. H.; Kushner, G. M.; Vickers, A. M.; Han, B.; Pei, P.; Stoner, G. D. *Clin. Cancer Res.* **2014**, *20*, 1910–1924.

(9) El-Bayoumy, K.; Chen, K. M.; Zhang, S. M.; Sun, Y. W.; Amin, S.; Stoner, G.; Guttenplan, J. B. *Chem. Res. Toxicol.* **2017**, *30*, 126–144.

(10) Petersen, P. E.; Bourgeois, D.; Ogawa, H.; Estupinan-Day, S.; Ndiaye, C. *Bull. World*

Health Organ. **2005**, *83*, 661–669.

(11) Ferlay, J.; Soerjomataram, I.; Dikshit, R.; Eser, S.; Mathers, C.; Rebelo, M.; Parkin, D. M.; Forman, D.; Bray, F. *Int. J. Cancer* **2015**, *136*, E359–E386.

(12) Bsoul, S.; Huber, M. A.; Terezhalmy, G. T. *J. Contemp. Dent. Pract.* **2005**, *6*, 1–16.

(13) Casto, B. C.; Knobloch, T. J.; Weghorst, C. M. In *Berries and Cancer Prevention*; Stoner, G. D.; Seeram, N., Eds.; Springer Science+Business Media: New York, NY, 2011; pp. 189–207.

(14) Howard, L. R.; Prior, R. L.; Liyanage, R.; Lay, J. O. *J. Agric. Food Chem.* **2012**, *60*, 6678–6693.

(15) Hager, A.; Howard, L. R.; Prior, R. L.; Brownmiller, C. *J. Food Sci.* **2008**, *73*, H134–H140.

(16) Gu, J.; Ahn-Jarvis, J.; Riedl, K. M.; Schwartz, S. J.; Clinton, S. K.; Vodovotz, Y. *J Agric Food Chem* **2014**, *62*, 3997–4006.

(17) Manach, C.; Hubert, J.; Llorach, R.; Scalbert, A. *Mol. Nutr. Food Res.* **2009**, *53*, 1303–1315.

(18) Thévenot, E. A.; Roux, A.; Xu, Y.; Ezan, E.; Junot, C. *J. Proteome Res.* **2015**, *14*, 3322–3335.

(19) Kemsley, E. K.; Le Gall, G.; Dainty, J. R.; Watson, A. D.; Harvey, L. J.; Tapp, H. S.; Colquhoun, I. J. *Br. J. Nutr.* **2007**, *98*, 1–14.

(20) Han, C.; Ding, H.; Casto, B.; Stoner, G. D.; D'Ambrosio, S. M. *Nutr. Cancer* **2005**, *51*, 207–217.

(21) Ding, H.; Han, C.; Guo, D.; Chin, Y. W.; Ding, Y.; Kinghorn, A. D.; D'Ambrosio, S. M. *Nutr. Cancer* **2009**, *61*, 348–356.

(22) Lee, H.; Li, D.; Prior, T.; Casto, B. C.; Weghorst, C. M.; Shuler, C. F.; Milo, G. E. *Med. Biochem.* **1997**, *13*, 419–434.

(23) Bishayee, A.; Haskell, Y.; Do, C.; Siveen, K. S.; Mohandas, N.; Sethi, G.; Stoner, G. D. *Crit. Rev. Food Sci. Nutr.* **2016**, *56*, 1753–1775.

(24) Cevallos-Cevallos, J. M.; Reyes-De-Corcuera, J. I.; Etxeberria, E.; Danyluk, M. D.; Rodrick, G. E. *Trends Food Sci. Technol.* **2009**, *20*, 557–566.

(25) Ronningen, I.; Miller, M.; Xia, Y.; Peterson, D. G. *J. Agric. Food Chem. ePub ahead*.

(26) Ronningen, I.; Peterson, D. G. *J. Agric. Food Chem.* **2018**, *66*, 682–688.

(27) Wishart, D. S.; Jewison, T.; Guo, A. C.; Wilson, M.; Knox, C.; Liu, Y.; Djoumbou, Y.; Mandal, R.; Aziat, F.; Dong, E.; Bouatra, S.; Sinelnikov, I.; Arndt, D.; Xia, J.; Liu, P.; Yallou, F.; Bjorndahl, T.; Perez-Pineiro, R.; Eisner, R.; Allen, F.; Neveu, V.; Greiner, R.; Scalbert, A. *Nucleic Acids Res.* **2013**, *41*, 801–807.

(28) Sumner, L. W.; Samuel, T.; Noble, R.; Gmbh, S. D.; Barrett, D.; Beale, M. H.; Hardy, N.; Harnly, J.; Higashi, R.; Kopka, J.; Lane, A. N.; Lindon, J.; Marriott, P.; Nicholls, A. W.; Reily, M. D.; Thaden, J. J.; Viant, M. R. *Metabolomics* **2007**, *3*, 211–221.

(29) Kula, M.; Majdan, M.; Głód, D.; Krauze-Baranowska, M. *J. Food Compos. Anal.* **2016**, *52*, 74–82.

(30) Van Der Sluis, A. A.; Dekker, M.; Van Boekel, M. A. J. S. *J. Agric. Food Chem.* **2005**, *53*, 1073–1080.

(31) Brownmiller, C.; Howard, L. R.; Prior, R. L. *J. Agric. Food Chem.* **2009**, *57*, 1896–1902.

(32) Gu, L.; Kelm, M. A.; Hammerstone, J. F.; Beecher, G.; Holden, J.; Haytowitz, D.; Prior, R. L. *J. Agric. Food Chem.* **2003**, *51*, 7513–7521.

(33) Stintzing, F. C.; Carle, R. *Trends Food Sci. Technol.* **2004**, *15*, 19–38.

(34) Totlani, V. M.; Peterson, D. G. *J. Agric. Food Chem.* **2005**, *53*, 4130–4135.

(35) Kokkinidou, S.; Peterson, D. G. *Food Funct.* **2013**, *4*, 1093.

(36) Srivastava, A.; Akoh, C. C.; Yi, W.; Fischer, J.; Krewer, G. *J. Agric. Food Chem.* **2007**, *55*, 2705–2713.

(37) Wang, L.; Hecht, S. S.; Carmella, S. G.; Yu, N.; Larue, B.; Henry, C.; Mcintyre, C.; Rocha, C.; Lechner, J. F.; Stoner, G. D. *Cancer Prev. Res.* **2009**, *2*, 84–93.

(38) Paudel, L.; Wyzgoski, F. J.; Giusti, M. M.; Johnson, J. L.; Rinaldi, P. L.; Scheerens, J. C.; Chanon, A. M.; Bomser, J. A.; Miller, A. R.; Hardy, J. K.; Reese, R. N. *J. Agric. Food Chem.* **2014**, *62*, 1989–1998.

(39) Rothwell, J. A.; Perez-Jimenez, J.; Neveu, V.; Medina-Rem??n, A.; M'Hiri, N.; Garc??a-Lobato, P.; Manach, C.; Knox, C.; Eisner, R.; Wishart, D. S.; Scalbert, A. *Database* **2013**, *2013*, 1–8.

(40) Tulio, A. Z.; Reese, R. N.; Wyzgoski, F. J.; Rtnaldi, P. L.; Fu, R.; Scheerens, J. C.; Miller, A. R. *J. Agric. Food Chem.* **2008**, *56*, 1880–1888.

(41) Torre, L. C.; Barritt, B. H. *J. Food Sci.* **1977**, *42*, 488–490.

(42) Patras, A.; Brunton, N. P.; O'Donnell, C.; Tiwari, B. K. *Trends Food Sci. Technol.* **2010**, *21*, 3–11.

(43) Zhang, Y. J.; Seeram, N. P.; Lee, R.; Feng, L.; Heber, D. *J. Agric. Food Chem.* **2008**, *56*, 670–675.

(44) Tanaka, T.; Tanaka, T.; Tanaka, M. *J. Exp. Clin. Med.* **2011**, *3*, 27–33.

(45) Hou, D.-X.; Kai, K.; Li, J.-J.; Lin, S.; Terahara, N.; Wakamatsu, M.; Fujii, M.; Young, M. R.; Colburn, N. *Carcinogenesis* **2003**, *25*, 29–36.

(46) Kay, C. D.; Kroon, P. A.; Cassidy, A. *Mol. Nutr. Food Res.* **2009**, *53*, 92–101.

Figure 1. Summary of untargeted metabolomics data pre-treatment and analysis.

Figure 2. Principal component analysis of all samples colored by storage temperature and labeled according to length of storage.

Figure 3. Heat map of molecular features with VIP>1 in PLS models for storage at 4–35 °C. Features were clustered using Euclidian distance metrics and Ward's linkage rule. * Denotes potential Maillard-related sugar fragmentation-phenolic degradation products determined after derivatization with *o*-phenylenediamine.

Figure 4. Growth inhibition of SCC-83-01-82 cells by extracts of BRB nectar stored at increasing temperatures. ANOVA terms for storage time, temperature, and their interaction were significant ($P<0.01$). Only significant differences within each storage temperature are denoted (*).

Figure 5. Averaged relative abundances of C3R and PA over time in each storage condition.

Figure 6. Dose-response relationship between increasing levels of C3R (A) and PA (B) and growth inhibition of SCC-83-01-82 cells. (C) When the ratio of C3R and PA were varied in equimolar solutions (molarity on right y-axis), growth inhibition (left y-axis) was maintained ($P = 0.092$ for differences among treatments).

Table 1. BRB nectar beverage formulation

Ingredients	% Wet Basis
Water	89.9
Sucrose	3.0
Pectin	0.5
Corn Syrup	1.0
BRB Powder	5.6
TOTAL	100.0

Table 2. PLS model cross validation results

Storage Temperature	Q^2	$P\,Q^2$	RMSEE
-20 °C	0.165	0.03	6.98
4 °C	0.948	0.01	1.04
10 °C	0.980	0.01	1.58
25 °C	0.919	0.01	0.997
35 °C	0.985	0.01	2.05

Table 3. Level 1 and 2 identified compounds from list of features with VIP>1 across all four PLS models

Compound Name	Molecular Formula	Retention time (min)	$[M-H]^-$	Δppm	Heat map cluster
Epicatechin[1]	$C_{15}H_{14}O_6$	3.6	289.0718	0	B
Catechin[1]	$C_{15}H_{14}O_6$	3.3	289.0718	0	B
B-type procyanidin dimer A[2]	$C_{30}H_{26}O_{12}$	3.6	577.1344	1	B
B-type procyanidin dimer B[2]	$C_{30}H_{26}O_{12}$	3.4	577.1398	8	B
Protocatechuic acid[1]	$C_7H_6O_4$	2.9	153.0196	2	C

[1] Level 1 identified features, [2] Level 2 identified features

Table 4. Quantitative analysis of C3R and PA in nectar from t_0 and 60 days at 35 °C

Time (d)	C3R (µg/mg extract)	PCA (µg/mg extract)
0	8.02 ± 0.20	$3.27 \times 10^{-2} \pm 8.1 \times 10^{-3}$
60	$0.20 \pm 5.7 \times 10^{-4}$	2.33 ± 0.13

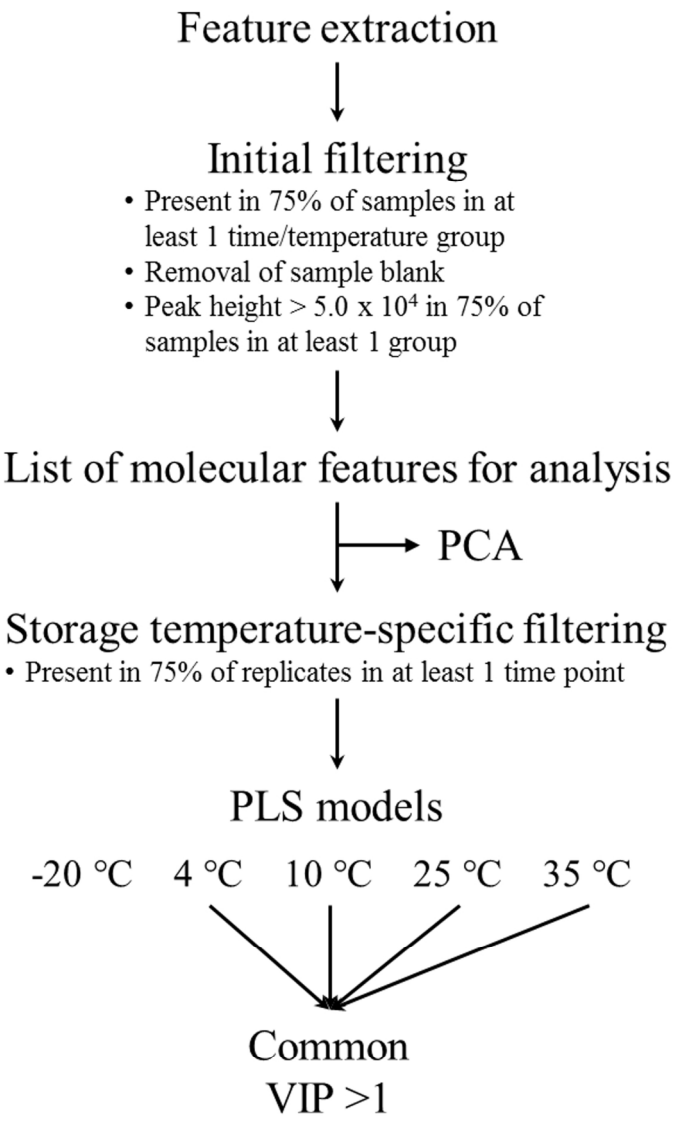

Figure 1. Summary of untargeted metabolomics data pre-treatment and analysis.

127x169mm (300 x 300 DPI)

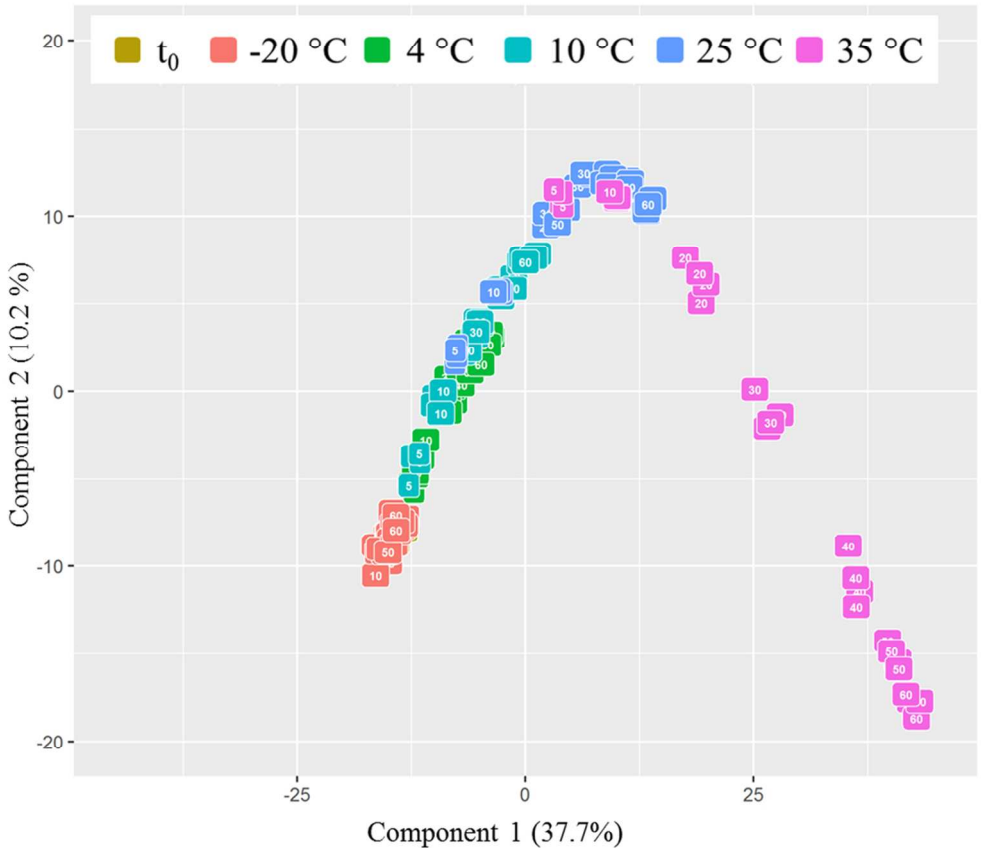

Figure 2. Principal component analysis of all samples colored by storage temperature and labeled according to length of storage.

101x101mm (300 x 300 DPI)

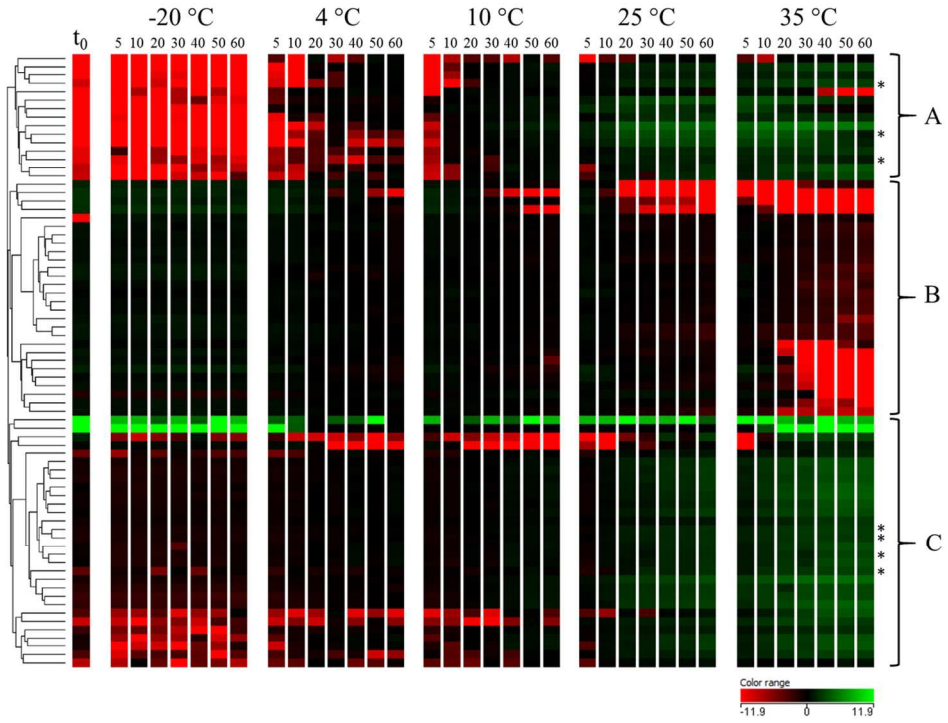

Figure 3. Heat map of molecular features with VIP>1 in PLS models for storage at 4–35 °C. Features were clustered using Euclidian distance metrics and Ward's linkage rule. * Denotes potential Maillard-related sugar fragmentation-phenolic degradation products determined after derivatization with o-phenylenediamine.

134x101mm (300 x 300 DPI)

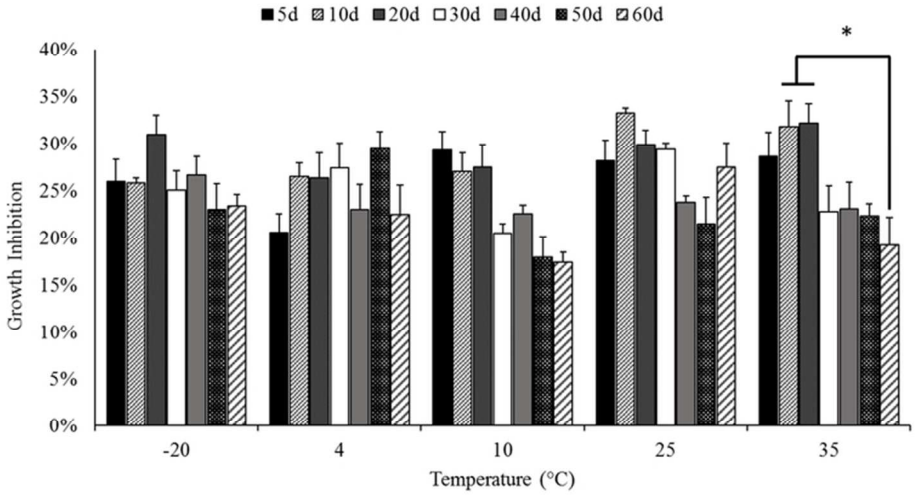

Figure 4. Growth inhibition of SCC-83-01-82 cells by extracts of BRB nectar stored at increasing temperatures. ANOVA terms for storage time, temperature, and their interaction were significant ($P<0.01$). Only significant differences within each storage temperature are denoted (*).

69x38mm (300 x 300 DPI)

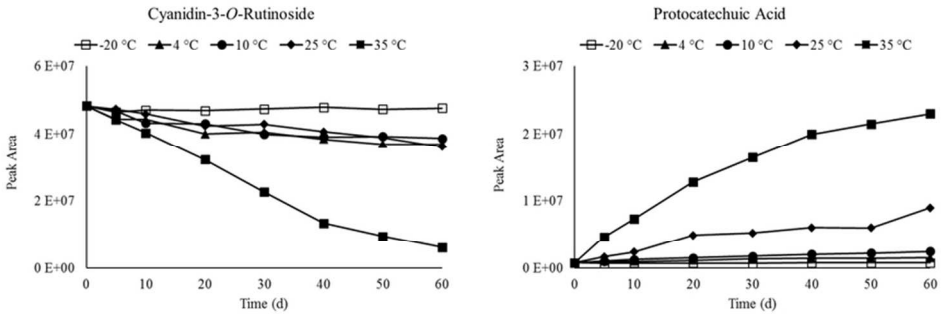

Figure 5. Averaged relative abundances of C3R and PA over time in each storage condition.

77x29mm (300 x 300 DPI)

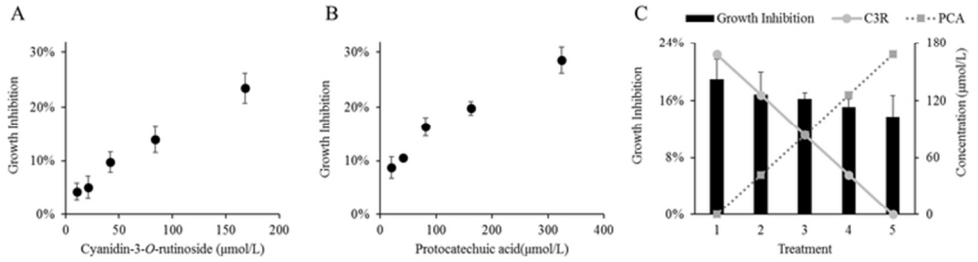

Figure 6. Dose-response relationship between increasing levels of C3R (A) and PA (B) and growth inhibition of SCC-83-01-82 cells. (C) When the ratio of C3R and PA were varied in equimolar solutions (molarity on right y-axis), growth inhibition (left y-axis) was maintained (P = 0.092 for differences among treatments).

66x21mm (300 x 300 DPI)

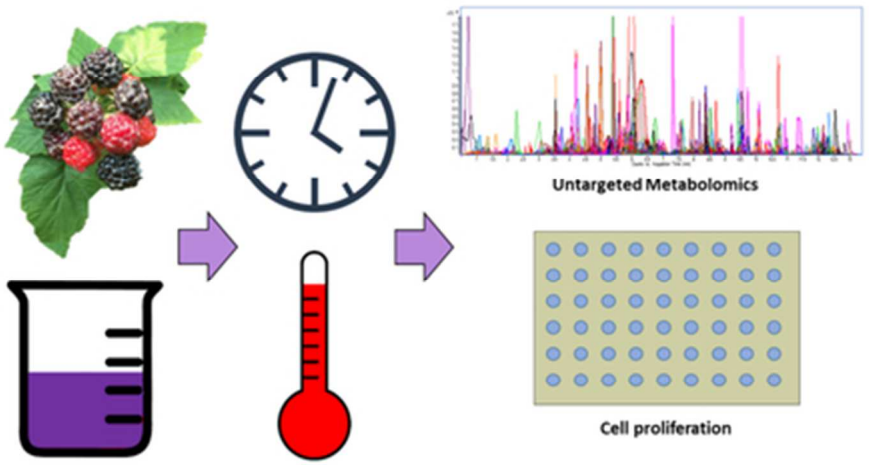

39x21mm (300 x 300 DPI)